Supporting information for

An on-site and portable electrochemical sensing platform based on spinel zinc ferrite nanoparticles for the quality control of paracetamol in pharmaceutical samples

Nguyen Tuan Anh[+1,*], Le Minh Tung[+3,**], Le Khanh Vinh[4], Nguyen Van Quy[5], Ong Van Hoang[1,6], Ngo Xuan Dinh[1], Anh-Tuan Le[1,2,***]

(1) Phenikaa University Nano Institute (PHENA), PHENIKAA University, Hanoi 12116, Vietnam

(2) Faculty of Materials Science and Engineering, PHENIKAA University, Hanoi 12116, Vietnam

(3) Department of Physics, Tien Giang University, My Tho city, Tien Giang Province, Vietnam

(4) National Institute of Applied Mechanics and Informatics, Vietnam Academy of Science and Technology (VAST), Ho Chi Minh 70000, Vietnam

(5) International Training Institute for Materials Science (ITIMS), Hanoi University of Science and Technology (HUST), 01 Dai Co Viet Road, Hanoi 10000, Vietnam

(6) University of Transport Technology, Trieu Khuc, Thanh Xuan District, Hanoi, Viet Nam

Corresponding authors:

*anh.nguyentuan1@phenikaa-uni.edu.vn (N.T. Anh)

**leminhtung@tgu.edu.vn (M.T. Le)

***tuan.leanh@phenikaa-uni.edu.vn (A.-T. Le)

[+] N.T. Anh and L.M Tung contributed equally to this work

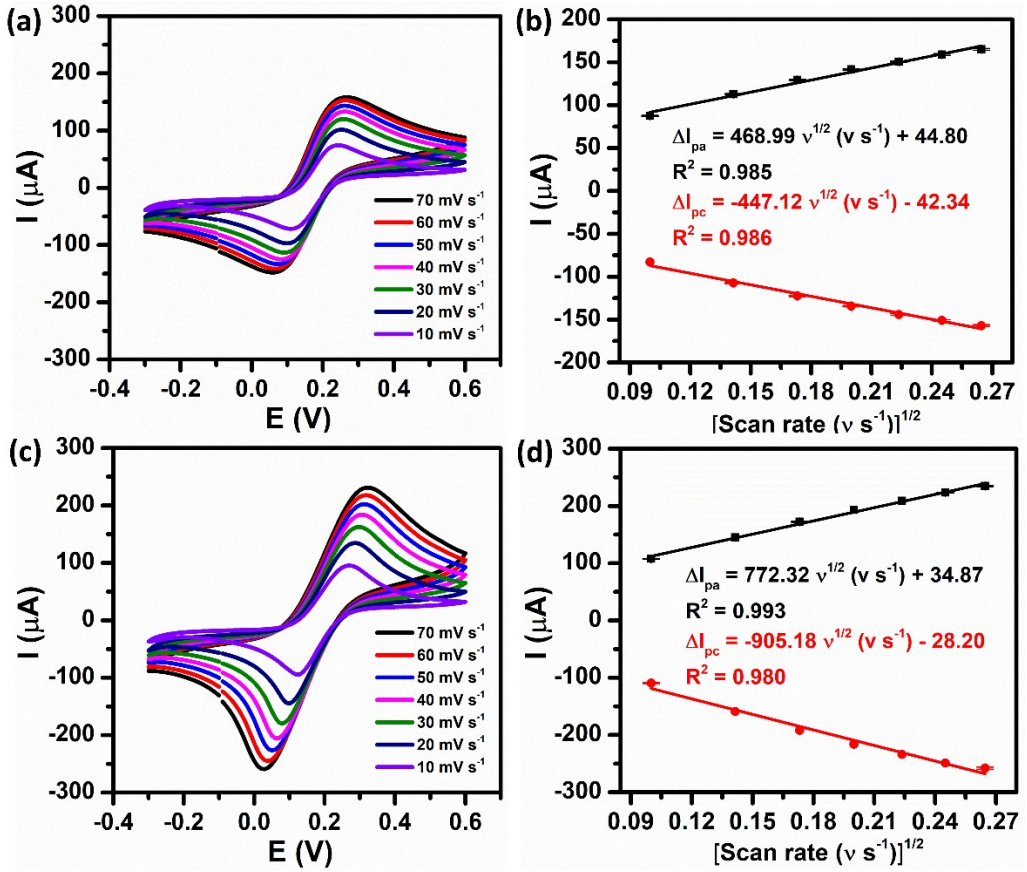

Fig. S1. CV responses of the bare SPE and $ZnFe_2O_4$/SPE in 5 mM $[Fe(CN)_6]^{3-/4-}$ containing 0.1 M KCl at different scan rates from 10 to 70 mV s^{-1} (a and c) and the corresponding calibration plots of peak current response *vs.* square root of scan rate (b and d), respectively.

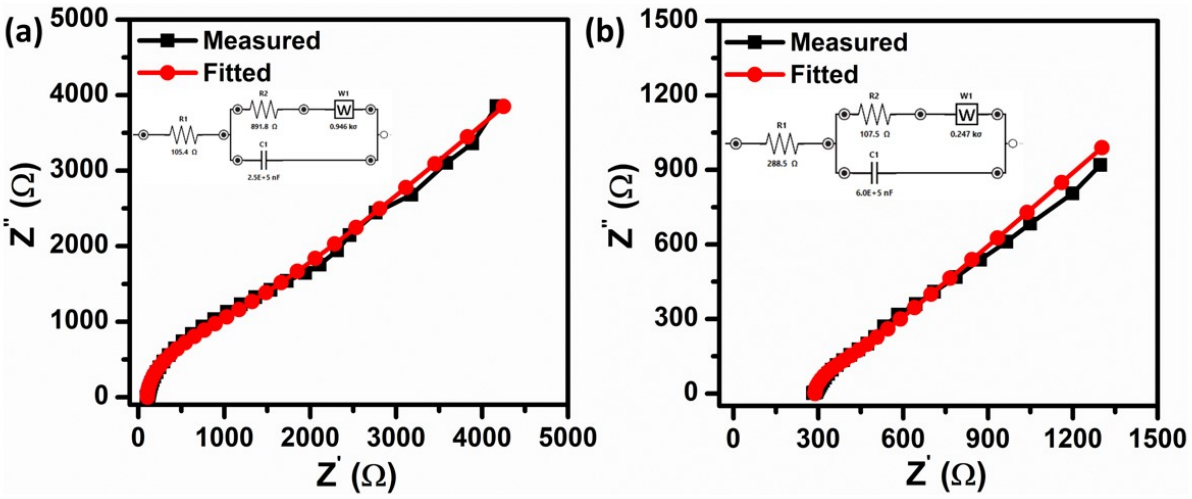

Fig. S2. Experimental and fitted Nyquist plots of the bare SPE (a) and $ZnFe_2O_4$/SPE (b) in the frequency range from 0.01 kHz to 00 kHz. Inset shows the Randles equivalent circuit used for fitting the data.

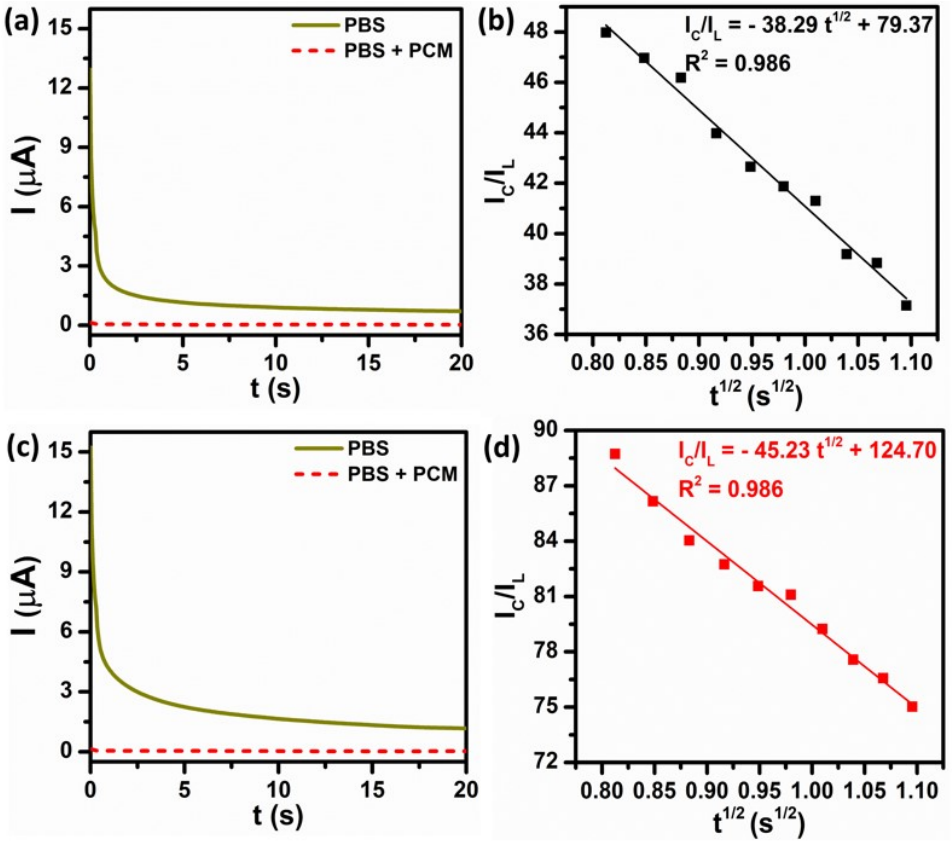

Fig. S3. Chronoamperometric response and plot of I_C/I_L *vs.* $t^{1/2}$ acquired from the chronoamperograms of the bare SPE (a and b) and $ZnFe_2O_4$/SPE (c and d) in the absence and presence of 500 μM PCM in 0.1 M PBS (pH 5.0).

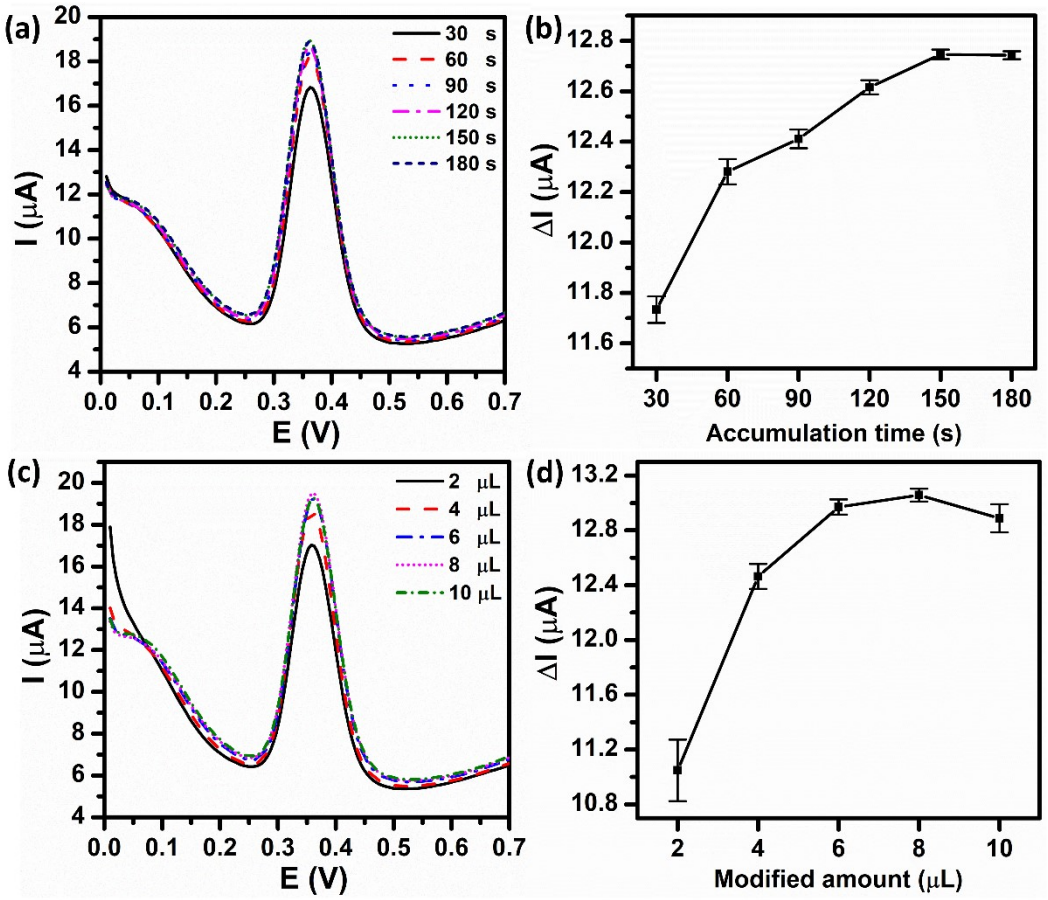

Fig. S4. Effect of accumulation time (a,b) and modified amount (c,d) on the PCM oxidation peak current of the $ZnFe_2O_4$/SPE.

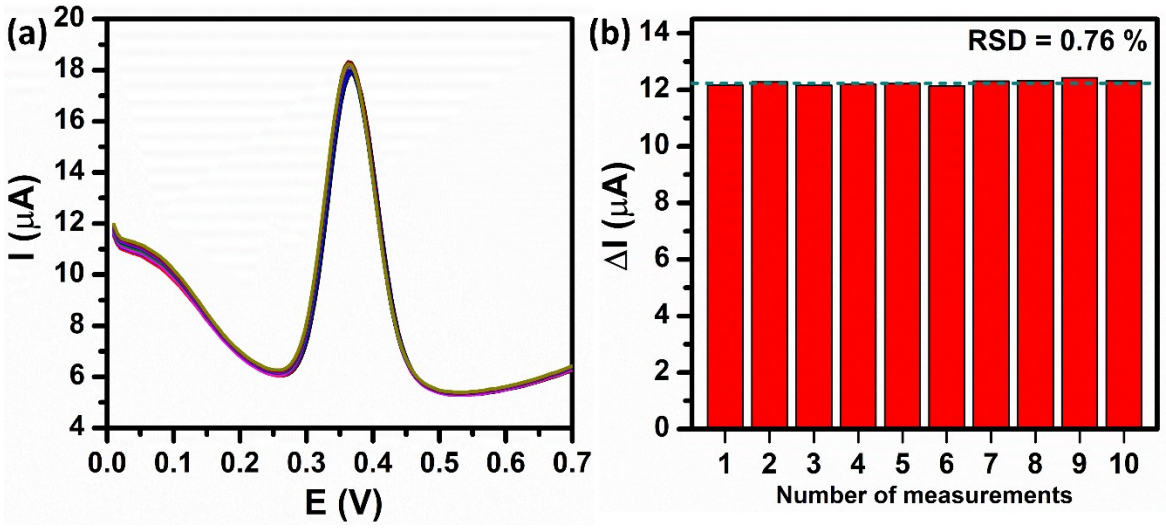

Fig. S5. Repeatability of the $ZnFe_2O_4$/SPE in 250 μM PCM.

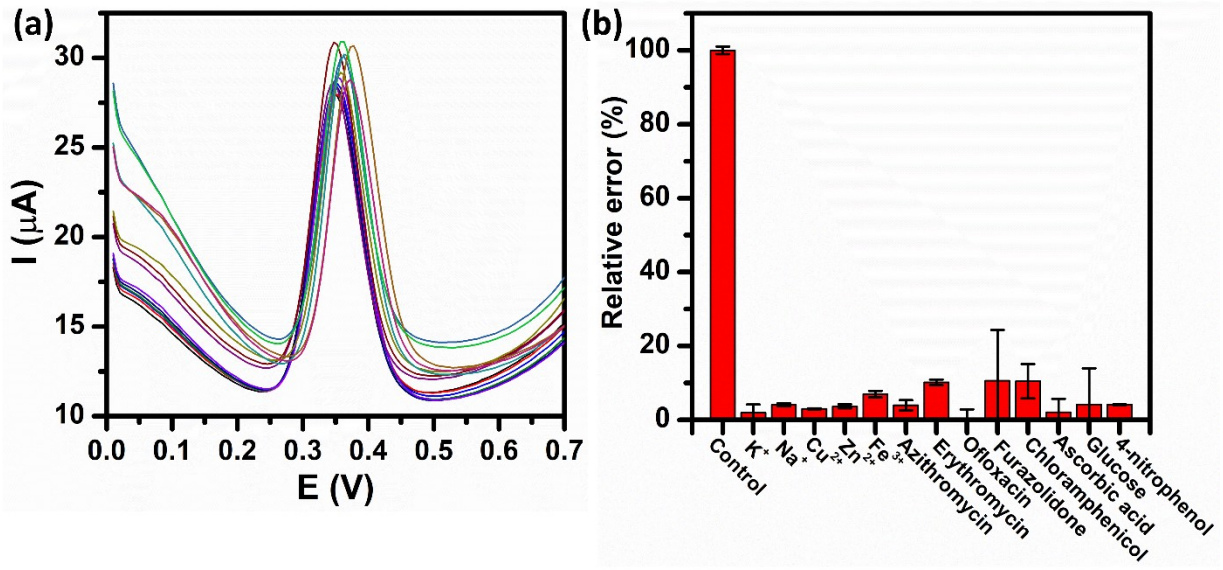

Fig. S6. Interference investigation of the $ZnFe_2O_4$/SPE in 0.1 M PBS (pH 5.0) containing 250 μM PCM with 10-fold concentration of interference substances.

Table S1 *Comparative study of the performance of various modified electrodes for PCM electrochemical detection* [a]

Modified Electrodes	Techniques	Analytical ranges (µM)	Limit of detection (µM)	Ref.
C60/GCE	DPV	50 – 1500	5	[1]
Cobalt hydroxide NPs/GCE	Amperometry	50 – 550	1.83	[2]
Fe_2O_3/CPE	DPV	2 – 150	1.16	[3]
ZrO_2/CPE	CV	10 – 60	0.68	[4]
CDA/Au-Ag/GCE	Amperometry	10 – 100	2.6	[5]
PAY/nano TiO_2/GCE	DPV	12 - 120	2.0	[6]
AuNP-PGA/SWCNTs	DPV	8.3 – 145.6	1.18	[7]
Ni-Al-HCF	Amperometry	3 – 1500	0.8	[8]
TiO_2/Graphene/GCE	DPV	1 – 100	0.21	[9]
$ZnFe_2O_4$ nanomaterials	DPV	0.5 – 400	0.29	This work

[a] GCE: glassy carbon electrode; CDA: cellulose diacetate; CPE: carbon paste electrode; PAY : poly(acid yellow 9); PGA: poly-glutamic acid; SWCNTs: single-walled carbon nanotubes; Ni-Al-HCF: hexacyanoferate(III) intercalated Ni Al layered double hydroxide

Table S2 *Comparative study of the performance of various techniques for the detection of PCM* [b]

Techniques	Analytical ranges	Limit of detection	Real samples	Ref.
HPLC	0.409 – 400 μg mL^{-1}	0.409 μg mL^{-1}	-	[10]
RP-HPLC	20 – 80 μg mL^{-1}	6 ng mL^{-1}	Tablet	[11]
Colorimetric method	25 – 400 mg mL^{-1}	-	Plasma	[12]
Chemiluminescence	0.025 – 0.25 μM	0.01 μM	Pharmaceuticals	[13]
Fluorescence	0.067 – 233 μg L^{-1}	0.022 μg L^{-1}	Human serum	[14]
UV-spectrophotometric	2 – 64 μg mL^{-1}	0.591 μg mL^{-1}	Tablet	[15]
Transmission FTIR spectroscopy	0.005 – 1 mg mL^{-1}	0.005 mg mL^{-1}	Tablets and capsules	[16]
FI – CE	6.2 – 200 μg mL^{-1}	0.7 μg mL^{-1}	Tablet	[17]
Electrochemical sensor	0.5 – 400 μM	0.29 μM	Tablet and human urine	This work

[b] HPLC: High-performance liquid chromatography; RP-HPLC: Reverse phase High-performance liquid chromatography; FTIR: Fourier transform infrared; FI – CE: flow injection-capillary electrophoresis.

References

1 R. N. Goyal and S. P. Singh, *Electrochim. Acta*, 2006, **51**, 3008–3012.

2 M. Houshmand, A. Jabbari, H. Heli, M. Hajjizadeh and A. A. Moosavi-Movahedi, *J. Solid State Electrochem.*, 2008, **12**, 1117–1128.

3 M. M. Vinay and Y. A. Nayaka, *J. Sci. Adv. Mater. Devices*, 2019, **4**, 442–450.

4 S. B. Matt, S. Raghavendra, M. Shivanna, M. Sidlinganahalli and D. M. Siddalingappa, *J. Inorg. Organomet. Polym. Mater.*, 2021, **31**, 511–519.

5 R. Wei, *Int. J. Electrochem. Sci.*, 2017, **12**, 9131–9140.

6 S. A. Kumar, C.-F. Tang and S.-M. Chen, *Talanta*, 2008, **76**, 997–1005.

7 M.-P. N. Bui, C. A. Li, K. N. Han, X.-H. Pham and G. H. Seong, *Sensors Actuators B Chem.*, 2012, **174**, 318–324.

8 K. Asadpour-Zeynali and R. Amini, *Electroanalysis*, 2017, **29**, 635–642.

9 Y. Fan, J.-H. Liu, H.-T. Lu and Q. Zhang, *Colloids Surfaces B Biointerfaces*, 2011, **85**, 289–292.

10 M. L. Altun, *Turkish J. Chem.*, 2002, **26**, 521–528.

11 P. R. Battu and M. S. Reddy, *Asian J. Res. Chem.*, 2009, **2**, 70–72.

12 F. Shihana, D. Dissanayake, P. Dargan and A. Dawson, *Clin. Toxicol.*, 2010, **48**, 42–46.

13 D. Easwaramoorthy, Y.-C. Yu and H.-J. Huang, *Anal. Chim. Acta*, 2001, **439**, 95–100.

14 X. Liu, W. Na, H. Liu and X. Su, *Biosens. Bioelectron.*, 2017, **98**, 222–226.

15 G. Murtaza, S. A. Khan, A. Shabbir, A. Mahmood, M. Asad, K. Farzana, N. S. Malik and I. Hussain, *Sci. Res. Essays*, 2011, **6**, 417–421.

16 M. A. Mallah, S. T. H. Sherazi, M. I. Bhanger, S. A. Mahesar and M. A. Bajeer, *Spectrochim. Acta Part A Mol. Biomol. Spectrosc.*, 2015, **141**, 64–70.

17 X. Liu, L. Liu, H. Chen and X. Chen, *J. Pharm. Biomed. Anal.*, 2007, **43**, 1700–1705.